Extremophiles (2017) 21:903–917
DOI 10.1007/s00792-017-0952-0

ORIGINAL PAPER

Gene regulation of two ferredoxin:NADP$^+$ oxidoreductases by the redox-responsive regulator SurR in *Thermococcus kodakarensis*

Ryota Hidese[1] · Keita Yamashita[1] · Kohei Kawazuma[1] · Tamotsu Kanai[2,3] · Haruyuki Atomi[2,3] · Tadayuki Imanaka[3,4] · Shinsuke Fujiwara[1,5]

Received: 29 August 2016 / Accepted: 2 July 2017 / Published online: 7 July 2017

Abstract The redox-responsive regulator SurR in the hyperthermophilic archaea *Pyrococcus furiosus* and *Thermococcus kodakarensis* binds to the SurR-binding consensus sequence (SBS) by responding to the presence of elemental sulfur. Here we constructed a *surR* gene disruption strain (DTS) in *T. kodakarensis*, and identified the genes that were under SurR control by comparing the transcriptomes of DTS and parent strains. Among these genes, transcript levels of ferredoxin:NADP$^+$ oxidoreductases 1 and 2 (FNOR1 and FNOR2) genes displayed opposite responses to *surR* deletion, indicating that SurR repressed *FNOR1* transcription while enhancing *FNOR2* transcription. Each promoter region contains an SBS upstream (uSBS) and downstream (dSBS) of TATA. In addition to in vitro binding assays, we examined the roles of each SBS in vivo. In *FNOR1*, mutations in either one of the SBSs resulted in a complete loss of repression, indicating that the presence of both SBSs was essential for repression. In *FNOR2*, uSBS indeed functioned to enhance gene expression, whereas dSBS functioned in gene repression. SurR bound to uSBS2 of *FNOR2* more efficiently than to dSBS2 in vitro, which may explain why SurR overall enhances *FNOR2* transcription. Further analyses indicated the importance in the distance between uSBS and TATA for transcriptional activation in *FNOR2*.

Keywords Transcriptional regulator · Redox-responsive · Regulation mechanism · Hyperthermophile · Archaea

Communicated by S. Albers.

Electronic supplementary material The online version of this article (doi:10.1007/s00792-017-0952-0) contains supplementary material, which is available to authorized users.

✉ Shinsuke Fujiwara
fujiwara-s@kwansei.ac.jp

[1] Department of Bioscience, Graduate School of Science and Technology, Kwansei-Gakuin University, 2-1 Gakuen, Sanda, Hyogo 669-1337, Japan

[2] Department of Synthetic Chemistry and Biological Chemistry, Graduate School of Engineering, Kyoto University, Katsura, Nishikyo-ku, Kyoto 615-8510, Japan

[3] Japan Science and Technology Agency, Core Research of Evolutional Science and Technology, 7, Gobancho, Chiyoda-ku, Tokyo 102-0076, Japan

[4] The Research Organization of Science and Technology, Ritsumeikan University, Kusatsu, Shiga 525-8577, Japan

[5] Research Center for Intelligent Bio-Materials, Department of Bioscience, Graduate School of Science and Technology, Kwansei-Gakuin University, 2-1 Gakuen, Sanda, Hyogo 669-1337, Japan

Introduction

The basal transcription machinery in archaea consists of a multisubunit RNA polymerase (RNAP) and three basal transcription factors, TATA-binding protein (TBP), transcription factor E (TFE), and transcription factor B (TFB) (Reeve 2003; Jun et al. 2011; Werner and Grohmann 2011). TBP and TFB recognize archaeal promoters by binding to the TATA-Box and the TFB-responsive element (BRE), respectively, and then RNAP interacts with the TFB and TBP complex bound to the promoter to initiate transcription. TFE facilitates open complex formation during preinitiation by interacting with the RNAP stalk and clamp and single-stranded DNA in the transcription bubble (Blombach et al. 2016; Schulz et al. 2016). The archaeal transcription machinery is similar to the eukaryotic systems involving RNAPII apparatus (Grohmann and Werner

2011; Werner and Grohmann 2011); however, the known transcriptional regulators are bacterial type (Geiduschek and Ouhammouch 2005; Lipscomb et al. 2009; Leyn and Rodionov 2015; Gindner et al. 2014). Repression by some transcriptional regulators is considered to occur through the formation of a protein–DNA supercomplex that interferes with the binding of TBP and/or TFB to the BRE/TATA-Box, as is the case for Lrs14 of *Sulfolobus solfataricus* (Bell and Jackson 2000), and/or the recruitment of RNAP, as is the mechanism proposed for both *Thermococcus kodakarensis* Tgr (Kanai et al. 2007) and *Pyrococcus furiosus* Phr (Vierke et al. 2003). The transcriptional activator TFB-RF1 acts as a TFB recruitment factor by binding just upstream of the BRE in *P. furiosus* (Ochs et al. 2012). Tgr of *T. kodakarensis* and XacR of *Haloferax volcanii* (Johnsen et al. 2015) act as a transcriptional activator and repressor depending on the location of the binding site relative to the TATA-Box. On the other hand, BarR in *Sulfolobus tokodaii* activates the expression of its own gene, even though the BRE/TATA-Box is located at the border between two *barR*-binding sites (Liu et al. 2014). Based on these reports, there seems to be a general tendency for these archaeal transcriptional regulating factors to act as activators when bound upstream of the TATA-Box and repressors when bound downstream, but there is still a need to further examine the individual promoters to understand the respective regulation mechanisms.

SurR, which is an ArsR-type transcription regulator, was identified as a key regulator responsible for molecular hydrogen production through an elemental sulfur (S^0)-dependent redox switch of the CXXC motif in the hyperthermophilic archaeon *P. furiosus* (Lipscomb et al. 2009; Yang et al. 2010; Lipscomb et al. 2017), which can grow in the presence or absence of S^0, depending on the available carbon source (Fiala and Stetter 1986). This transcriptional regulator is widely conserved among the order Thermococcales. A reduced form of SurR acts as a transcriptional activator through binding to the SurR-binding consensus sequence (SBS, $GTTn_3AAC$) (Lipscomb et al. 2009). By contrast, an intramolecular disulfide bond is thought to form in the SurR CXXC motif in the presence of S^0, resulting in the loss of its ability to bind to the SBS (Yang et al. 2010). The expression of genes involved in hydrogen-generating respiration, including the *mbh* gene cluster, which encodes the components of membrane-bound hydrogenase (MBH), is activated by binding of a reduced form of SurR to the SBS in the absence of S^0. In turn, genes involved in H_2S-generating respiration, including *nsr*, the gene encoding NAD(P)H sulfur reductase, are derepressed by loss of the ability of the oxidized form of SurR to bind to the SBS in the presence of S^0. In *Thermococcus onnurineus* NA1, the redox state of SurR can be regulated by protein disulfide oxidoreductase and thioredoxin reductase couple (Lim et al. 2017). SurR is now considered as a master regulator of the primary electron flow pathways in the order Thermococcales (Lipscomb et al. 2017). This redox-responsive regulation dominated by a two cysteine-type thiol-based mechanism is also seen with several bacterial transcription factors, such as *Escherichia coli* OxyR and *Bacillus subtilis* Spx (Antelmann and Helmann 2011; Hillion and Antelmann 2015). Disruption of the *surR* gene of *T. kodakarensis* (*Tk-surR*) is lethal in the absence of S^0, consistent with the fact that *Tk*-SurR activates the expression of genes involved in molecular hydrogen production (Santangelo et al. 2011).

Although a wealth of structural and biochemical evidence has been obtained, genetic studies on SurR have been rather limited to the responses of the cell brought about by *surR* gene disruption. In the present study, we took advantage of the genetic tools developed for *T. kodakarensis* (Sato et al. 2003, 2005; Matsumi et al. 2007; Santangelo et al. 2008). We first perform a comparative transcriptome analysis with a *surR*-deleted mutant (DTS) of *T. kodakarensis* grown in the presence of S^0 to identify genes that are specifically under the control of *Tk*-SurR. We then proceed to examine the contributions of SBSs in the promoters of two genes under the control of SurR, ferredoxin:$NADP^+$ oxidoreductase 1 and 2 (FNOR1 and FNOR2), both in vitro and in vivo. The promoters of *FNOR1* and *FNOR2* each contain two SBSs, upstream and downstream of the TATA-Box. Our transcriptome analysis indicated that the transcript levels of these two genes displayed opposite responses to *surR* deletion even though both promoters display SBS:TATA-Box:SBS structures. Our analyses indicated that the locations of SBSs and the binding affinities of *Tk*-SurR toward the individual SBSs are key determinants in its transcriptional regulation.

Materials and methods

Microorganisms and media

Thermococcus kodakarensis KU216 (Δ*pyrF*) (Sato et al. 2005) and its derivatives (Table 1) were cultivated anaerobically in a nutrient-rich medium artificial seawater-yeast extract-tryptone (ASW-YT) (Atomi et al. 2004) containing 2.0 g L^{-1} S^0 or in synthetic medium (Sato et al. 2005) containing 0.8 × artificial seawater, amino acids, and S^0. For solid medium, 1% gelrite (Wako, Osaka, Japan) and 2 mL L^{-1} polysulfide solution (10 g of $Na_2S{\cdot}9H_2O$ and 3 g of sulfur flowers in 15 mL of H_2O) were added. *E. coli* strains were cultivated at 37 °C in LB medium containing 50 μg mL^{-1} ampicillin.

Table 1 Strains and primers used in this study

Strain or primer	Relevant characteristic(s) or sequence (5′–3′)	Source and reference
Strains		
E. coli		
BL21-CodonPlus(DE3)-RIL	F$^-$ *ompT hsdS*(r_B^- m_B^-) *dcm* + Tet^r gal λ *endA* Hte [*argU ileY leuW* Cam^r]	Agilent Technologies
DH5α	F$^-$ Φ80d*lacZ*ΔM15 Δ*lacZYA-argF*)U169 *deoR recA1 endA1 hsdR*17(r_K^-, m_K^+) *phoA supE44* λ^- *thi*-1 *gyrA*96 *relA*1	Takara Bio
T. kodakarensis		
KU216	Δ*pyrF*	Sato et al. (2005)
DAD	Δ*pyrF,* Δ*pdaD*	Fukuda et al. (2008)
DTS	Δ*pyrF,* Δ*surR*	This study
Primers		
TkSurR-Fw1	AAAAGGATCCCCCCCACCTGAGACTTCCTA	
TkSurR-Rv1	AAAAGAATTCCGGGTATGAGTCCGACATTT	
Inv-TkSurR-Fw	AAGGCGAAGCTGGGTGGTGAAACCGATGCC	
Inv-TkSurR-Rv	CAGTATGTAAAAGATGTCTGGTTCAGA	
TK1326-Fw	TCCATTATCCTTCCGTCGGGCTGAAAAACC	
TK1326-Rv	AAAAAAAACATATGAATGAACACCTCCGTA	
TK1685-Fw	TTCAGGGCTTTTCTGGTGAAAATTGGGGTT	
TK1685-Rv	AAAAAAAACATATGAGTGCACCACCTCGAACA	
F1-ΔuSBS1-Fw	TAAACCTTTGCCCAACAACAGGTTTATAA	
F1-ΔuSBS1-Rv	TTATAAACCTGTTGTTGGGCAAAGGTTTA	
F1-ΔdSBS1-Fw	AGCACTTAAACCGGTGGGGCTTTAGATGT	
F1-ΔdSBS1-Rv	ACATCTAAAGCCCCACCGGTTTAAGTGCT	
F1-ΔuSBS2-Fw	CTGGTGAAAATTGGGCCCCTAAACCTTTGGTTCAAAAAA	
F1-ΔuSBS2-Rv	TTTTTTGAACCAAAGGTTTAGGGGCCCAATTTTCACCAG	
F1-ΔdSBS2-Fw	GCGTATAAACCTTGAGGGCAACCCTAAAGGTGAACATAT	
F1-ΔdSBS2-Rv	ATATGTTCACCTTTAGGGTTGCCCTCAAGGTTTATACGC	
F2-uSBS2-Fw	GGGCTTTTCTGGTGAAAAGTTCTAAACCTTTGGTTTTGGGCAAAAAAAGCG TATAAACCTTGA	
F2-uSBS2-Rv	TCAAGGTTTATACGCTTTTTTTGCCCAAAACCAAAGGTTTAGAACTTTTCA CCAGAAAAGCCC	
F3-uSBS2-Fw	CAGGGCTTTTCTGGTGTTCTAAACCTTTGGTTGAAAATTGGGCAAAAAAAG CGTATAAACCTTGA	
F3-uSBS2-Rv	TCAAGGTTTATACGCTTTTTTTGCCCAATTTTCAACCAAAGGTTTAGAACA CCAGAAAAGCCCTG	
F4-uSBS2-Fw	TTTCTGGTGAAAATTGGGCAAAAGTTCTAAACCTTTGGTTAAAGCGTATAA ACCTTGA	
F4-uSBS2-Rv	TCAAGGTTTATACGCTTTAACCAAAGGTTTAGAACTTTTGCCCAATTTTCA CCAGAAA	
TK1326 sense primer	ATAGCCAGGGCCTGGCAGGA	
TK1326 antisense primer	CCTGACCTTGGCTGTGGCTC	
TK1685 sense primer	CGCACGTGGCCCGCTCTTGG	
TK1685 antisense primer	GCGGCCCGGCAACGCTCAGA	
tk_16S sense primer	GCCCCGAAACCCCCGGGCTACACGCGCGCT	
tk_16S antisense primer	CGTATTCGCCGCGCGATGATGACACGCGGG	
TkSurR-Fw	AAAAAAACATATGTCTGAACCAGACATCTT	
TkSurR-Rv	AGAATTCTTAATCTTCTCCGGCATCGGTTT	
TK1326-Fw2	TCCATTATCCTTCCGTCGGGCTGAAAAACC	
TK1685-Fw2	TTCAGGGCTTTTCTGGTGAAAATTGGGGTT	
IRD700-Rv	IRD700-CGGTCTATTCTTAGGTACAT	

Underlined sequences indicate restriction enzyme sites

Construction of the *surR*-deleted strain

The principles underlying specific gene disruption in *T. kodakarensis* have been described previously (Sato et al. 2005). The vector for disrupting the *surR* gene [954,255–954,965 (+) bp in the *T. kodakarensis* genome] through double-crossover homologous recombination was constructed as follows. A set of primers, TkSurR-Fw1/TkSurR-Rv1, was designed to amplify DNA fragments containing the *surR* gene along with its flanking regions (ca. 1000 bp each) by PCR using *T. kodakarensis* genomic DNA. The DNA fragment containing the *surR* gene was cloned into the *Bam*HI/*Eco*RI sites of pUD2 (Sato et al. 2005), yielding the plasmid pUD2-SurR. The coding region of *surR* was then removed using inverse PCR with the primers Inv-TkSurR-Fw/Inv-TkSurR-Rv, and the resultant PCR fragment was 5′-phosphorylated and self-ligated. The resulting disruption vector, pUD2-ΔSurR, was used for gene deletions in the host strain *T. kodakarensis* KU216 (Δ*pyrF*). Gene deletions were confirmed by nucleotide sequencing with an ABI PRISM® 3130 Genetic Analyzer (Thermo Fisher Scientific, Waltham, MA, USA).

Microarray analysis

KU216 and the *Tk*-SurR-deleted strain DTS (Δ*pyrF*, Δ*surR*) were individually cultivated at 85 °C in the presence and absence of S^0. Cells were harvested in mid-log phase, and total RNA was extracted using the RNeasy mini kit (Qiagen, Venlo, The Netherlands). The microarray plate used in this study (Array Tko2) was manufactured at Takara Bio (Otsu, Japan) and covers all 2306 genes of the *T. kodakarensis* genome. Two identical sets (left and right) are loaded on each plate. Therefore, two sets of data were obtained from each microarray plate. The results are the average of two independent microarray slides, and error bars represent standard deviation. The experimental procedure for microarray analysis is described elsewhere (Kanai et al. 2007).

Construction of the *FNOR1* and *FNOR2* promoter region variants

The principles underlying the promoter-probe analysis with the plasmid pTKR have been described previously (Nagaoka et al. 2013). The plasmid pTKR was constructed from pTK01 (Santangelo et al. 2008), a derivative of pTN1 (Soler et al. 2007). The pTKR harbors a promoter-less catalase gene from *Pyrobaculum calidifontis* (Amo et al. 2002). A DNA fragment containing the 5′-flanking region of *TK1326* or *TK1685* was amplified by PCR from *T. kodakarensis* genomic DNA using the primer set TK1326-Fw/TK1326-Rv or TK1685-Fw/TK1685-Rv, respectively. The amplified fragments were cloned into the *Eco*RV/*Nde*I sites of pTKR (Nagaoka et al. 2013), yielding pTKRF1 and pTKRF2, respectively. The *TK1326* promoter-probe plasmid variants (pTKRF1-1, pTKRF1-2, and pTKRF1-12) were obtained by QuikChange site-directed mutagenesis (Agilent Technologies, Santa Clara, CA) of pTKRF1 using specific primer sets (F1-ΔuSBS1-Fw/F1-ΔuSBS1-Rv for pTKRF1-1, F1-ΔdSBS1-Fw/F1-ΔdSBS1-Rv for pTKRF1-2, and both primer sets for pTKRF1-12). The *TK1685* promoter-probe plasmid variants (pTKRF2-1, pTKRF2-2, pTKRF2-12) were obtained by site-directed mutagenesis of pTKRF2 using specific primer sets (F1-ΔuSBS2-Fw/F1-ΔuSBS2-Rv for pTKRF2-1, F1-ΔdSBS2-Fw/F1-ΔdSBS2-Rv for pTKRF2-2, and both primer sets for pTKRF2-12) and the other *TK1685* promoter-probe plasmid variants (pTKRF2-3, pTKRF2-4, and pTKRF2-5) were obtained by the same way using specific primer sets (F2-uSBS2-Fw/F2-uSBS2-Rv for pTKRF2-3, F3-uSBS2-Fw/F3-uSBS2-Rv for pTKRF2-4, and F4-uSBS2-Fw/F4-uSBS2-Rv for pTKRF2-5).

Quantitative real-time PCR (qRT-PCR)

Total RNA was obtained from *T. kodakarensis* cells using the RNeasy mini kit, and qRT-PCR was performed using the Super-Script III RT/Platinum kit (Invitrogen, Carlsbad, CA, USA) and an ABI PRISM 7000 sequence detection system (Applied Biosystems, Foster City, CA, USA). Total RNA extracts were treated with DNase I following the manufacturer's instructions (Roche Applied Science, Penzberg, Germany). The primers used to amplify the *TK1326*, *TK1685*, and 16S rRNA genes by qRT-PCR were a TK1326 sense primer/TK1326 antisense primer, a TK1685 sense primer/TK1685 antisense primer, and a tk_16S sense primer/tk_16S antisense primer, respectively. Each sequence-specific standard curve was generated with varying amounts of PCR products, which were separately amplified from the *TK1326*, *TK1685*, and 16S rRNA genes with the corresponding primer set used in qRT-PCR. The mRNA levels shown are an average of three independent technical replicates and were normalized against the level of 16S rRNA, which was set to 1.

Expression and purification of *Tk*-SurR

The primers used to clone *surR* were TkSurR-Fw and TkSurR-Rv (Table 1). The amplified DNA fragment encoding *surR* was cloned into the *Nde*I/*Eco*RI sites of pET21a, yielding the plasmid pSurR. *E. coli* BL21-CodonPlus (DE3)-RIL cells harboring pSurR were grown in LB medium containing 100 μg mL^{-1} ampicillin at 37 °C for 6 h. After induction by treatment with 1 mM isopropyl-β-D-thiogalactopyranoside for 4 h, cells were harvested

by centrifugation at 10,000×*g* for 30 min, resuspended in Buffer A (20 mM Tris–Cl, 1 mM EDTA, 1 mM 2-mercaptoethanol, and 0.2 mM phenylmethylsulfonyl fluoride, pH 7.5), and disrupted by sonication. After removing cell debris by centrifugation at 23,000×*g* for 60 min, the supernatants were used for purification. The supernatant was incubated at 80 °C for 30 min and centrifuged (23,000×*g* for 60 min), and the resultant supernatant was applied to a HiTrap Q anion-exchange column (GE Healthcare, Little Chalfont, UK). *Tk*-SurR was eluted with a linear gradient of NaCl (0–1.0 M) prepared in Buffer A. Fractions containing *Tk*-SurR were confirmed by SDS-PAGE and collected. The protein concentration was determined by the Bradford assay using bovine serum albumin as a standard (Bradford 1976).

Circular dichroism (CD) spectroscopy

CD spectroscopic experiments were performed on a J-820 CD spectropolarimeter (JASCO) at 20 °C. Far-UV CD spectra in the 215–260 nm region were measured using a quartz cuvette (pathlength of 0.2 cm) at 0.05 nm steps over the wavelength range, with a scan speed of 50 nm min^{-1}. The experiments were performed with 1.8 μM *Tk*-SurR prepared in 50 mM potassium phosphate buffer (pH 7.4) in the presence of 5 mM dithiothreitol or 5 mM diamide. All samples were preincubated at room temperature for 30 min before each scan. All spectra were corrected for the contributions of buffer to the signals.

Gel-shift assay

The promoter regions of the *TK1326* and *TK1685* genes were amplified by PCR with the primer set TK1326-Fw2/IRD700-Rv (an IRD700-labeled primer) from the pTKRF1 plasmid and its derivatives or with the primer set TK1685-Fw2/IRD700-Rv from the pTKRF2 plasmid and its derivatives, respectively, producing IRD700-labeled DNA probes (Table 1). The complex between *Tk*-SurR and each free probe was detected by a mobility shift in a non-denaturing 5% polyacrylamide gel. Various concentrations of *Tk*-SurR were incubated with 2 nM IRD700-labeled DNA probe in 20 μL of binding buffer containing 20 mM Tris–HCl (pH 7.5), 15 mM KCl, 0.2% Tween 20, and 63 ng mL^{-1} salmon sperm for 30 min at 60 °C. After adding 0.25% bromophenol blue dye containing 40% sucrose to the reaction mixture, the complex was separated by electrophoresis on a 5% polyacrylamide gel in Tris–borate–EDTA electrophoresis buffer (45 mM Tris–borate, pH 8.0, and 1 mM EDTA). Signals were visualized with an Odyssey infrared imaging system (LI-COR Biosciences, Lincoln, NE, USA). Fractional saturation was determined at each protein concentration by densitometry of free DNA using NIH ImageJ software. The data were obtained from three independent experiments and fitted to the Hill equation (fraction bound = $[protein]^n/([protein]^n + K_d{}^n)$, where n is the Hill coefficient and K_d is the apparent dissociation constant, using Kaleida Graph software (Adelbeck Software, Reading, PA, USA).

Immunoblotting analysis

Cell extracts (20 μg of each) obtained by sonication were separated by SDS-PAGE and transferred to polyvinylidene difluoride membranes (ATTO, Tokyo, Japan). Immunodetection was performed with an antibody raised against *Pc*-Kat in rabbit and Alexa Fluor 700 goat anti-rabbit IgG (Invitrogen). Signals were visualized with an Odyssey infrared imaging system (LI-COR Biosciences).

Results

Transcriptome analysis

The *Tk-surR* gene-deleted strain, named *T. kodakarensis* DTS, was obtained by homologous recombination (Supplemental Fig. 1). Consistent with the growth property of the *T. kodakarensis* TS1101 strain (Δ*pyrF*, Δ*trpE::pyrF*, Δ*surR*) reported previously (Santangelo et al. 2011), the DTS strain did not grow in the absence of S^0. The reduced form of *Tk*-SurR is presumed to activate genes involved in hydrogen production by sequence-specific binding. In the present study, to identify genes whose expression is dependent on the regulation of *Tk*-SurR in the presence of S^0, a comparative transcriptome analysis was carried out using total RNA extracted from the *T. kodakarensis* DTS and KU216 strains. The transcriptome data are available under the number GSE71984 in the gene expression omnibus (GEO) database at NCBI (http://www.ncbi.nlm.nih.gov/geo/query/acc.cgi?acc=GSE71984). The genes whose transcript levels increased or decreased more than fourfold in the DTS strain in two independent experiments are listed in Tables 2 and 3, respectively. The transcript levels of eight genes were more than fourfold higher in the DTS strain than in the KU216 strain, including *TK1326*, which encodes a component of FNOR1 (Table 2). Among the eight genes, *TK0164–TK0166* and *TK1024–TK1025* constitute a gene cluster. On the other hand, the transcript levels of 37 genes were more than fourfold lower in the DTS strain than in the KU216 strain (Table 3). Among these down-shifted genes in the DTS strain, *TK2076–TK2077*, *TK2073–TK2075*, *TK2070–TK2072*, *TK2080–TK2093* (*TK2090* and *TK2092* were not detected in the analysis), *TK0038–TK0044*, and *TK0119–TK0121* are present in a gene cluster. The *TK2076–TK2077* genes, which are predicted to encode formate:ferredoxin oxidoreductase, were

Table 2 ORFs whose signal intensities were increased more than fourfold in the DTS strain compared with the KU216 strain

No.	Gene ID	Annotation	Mean intensity ratio* [$\log_2$(DTS/KU216) ± SD]
1	*TK0443*	Hypothetical membrane protein	2.01 ± 0.23
2	*TK1326*	Ferredoxin:NADP oxidoreductase, β subunit	2.12 ± 0.11
3	*TK1463*	Hypothetical protein, conserved	2.28 ± 0.03
4	*TK0164*	*S*-Layer-like array protein	2.36 ± 0.14
5	*TK1025*	Hypothetical protein, conserved, containing ATP/GTP-binding site motif A	2.64 ± 0.04
6	*TK1024*	Hypothetical membrane protein	2.69 ± 0.04
7	*TK0165*	Hypothetical protein	2.90 ± 0.19
8	*TK0166*	Hypothetical protein	3.12 ± 0.17

* The mean intensity ratio (DTS/KU216) is expressed as a $\log_2$ value with standard deviation (SD)

the most down-shifted in the DTS strain. The transcripts of *TK2080–TK2093*, which encode the components of MBH, decreased to less than one-sixteenth of the level observed in the KU216 strain. In addition, the expression levels of four genes, *TK1209*, *TK1481*, *TK0675*, and *TK1685*, which encode a transmembrane electron transport protein, an NADH:polysulfide oxidoreductase, a hypothetical protein belonging to the radical *S*-adenosylmethionine superfamily, and a component of FNOR2, respectively, decreased dramatically in the DTS strain.

SBSs ($GTTn_3AAC$) were found upstream of the *TK2076–TK2077*, *TK2080–TK2093*, *TK1481*, *TK1209*, *TK0675*, *TK1325*, and *TK1685* genes (Table 4). Furthermore, two SBSs were found in the upstream regions of the *TK0675*, *TK1325*, and *TK1685* genes. Based on a comprehensive identification of each transcription start site in *T. kodakarensis* obtained by differential RNA-sequencing analysis (Jäger et al. 2014), we predicted the TATA-Box sequence in the promoter region of each gene. According to the analysis, 18 bp is the average distance between the 3′-end of the nearest upstream SBS and the 5′-start point of the TATA-Box sequence in the five down-shifted genes, i.e., *TK2076–TK2077*, *TK1481*, *TK1209*, *TK0675*, and *TK1685*. The distance in the upstream region of the *TK2080–TK2093* gene cluster was exceptionally long at 47 bp. For efficient SurR binding, an extended motif has been proposed, which includes a second palindromic half-site with a 5 bp gap: $GTTn_3AACn_5GTT$ (Lipscomb et al. 2009). This extended motif was also found in the promoter regions of the *TK2080–TK2093* gene cluster and the *TK1481*, *TK1209*, *TK0675*, and *TK1685* genes. We also identified a number of genes that although responding to *Tk-surR* deletion, did not harbor SBSs in their promoter regions at least up to 200 bp. These were the *TK2073–TK2075*, *TK0038–TK0044*, and *TK0119–TK0121* gene clusters, and the *TK2079*, *TK0631*, and *TK0842* genes. These genes are most likely regulated by factors that are under the control of *Tk*-SurR and not directly recognized by *Tk*-SurR itself.

The different expression profiles of two *FNOR* genes

Our transcriptome analysis showed that the transcript level of *TK1685* decreased, whereas that of *TK1326* increased in the DTS strain. Both genes encode FNOR isozymes (Santangelo et al. 2011). *TK1326–TK1325* and *TK1685–TK1684* encode the β- and α-subunits of two FNORs, designated here as FNOR1 and FNOR2, respectively. FNOR1 and FNOR2 are 60% identical to each other. We measured the mRNA levels of these two genes in the KU216 strain grown in the presence or absence of S^0 and in the DTS strain grown in the presence of S^0 using qRT-PCR (Fig. 1). The transcript levels of *TK1326* and *TK1685* were about fivefold and 1.6-fold higher in the KU216 strain grown in the presence of S^0 than in that grown in the absence of S^0, respectively. The transcript levels of *TK1326* (*FNOR1*) in the DTS strain were twofold higher than in the KU216 strain, whereas those of *TK1685* (*FNOR2*) were twofold lower in the DTS strain than in the KU216 strain (Fig. 1a, b). The results indicate that in strain KU216, transcripts of both FNOR1 (*TK1326*) and FNOR2 (*TK1685*) increase in the presence of S^0 (Fig. 1), but the genes respond differently to *Tk-surR* disruption. Although the tendencies were the same, the mean intensity ratios [*TK1326* of $\log_2$(DTS/KU216) = 2.12; *TK1685* of $\log_2$(DTS/KU216) = −2.06] obtained by our DNA microarray analysis differed from the fold changes calculated by qRT-PCR analysis (Tables 2, 3; Fig. 1). This may be due to low levels of transcripts of the oxidoreductase genes, resulting in low hybridization efficiency and non-specific hybridization and/or cross-hybridization in the DNA microarray analysis (Koltai and Weingarten-Baror 2008). Quantification of the transcripts achieved by qRT-PCR

Table 3 ORFs whose signal intensities were decreased more than fourfold in the DTS strain compared with the KU216 strain

No.	Gene ID	Annotation	Mean intensity ratio [$\log_2$(DTS/KU216) ± SD][a]
1	*TK2077*	Formate:ferredoxin oxidoreductase, 4Fe–4S cluster-binding β subunit	−5.52 ± 0.16
2	*TK2074*	Glutamate synthase β chain-related oxidoreductase	−5.22 ± 0.20
3	*TK2089*	Membrane-bound hydrogenase, NiFe-hydrogenase small subunit	−5.22 ± 0.02
4	*TK2086*	Membrane-bound hydrogenase, MbhG subunit	−5.14 ± 0.25
5	*TK2084*	Membrane-bound hydrogenase, MbhE subunit	−5.13 ± 0.06
6	*TK2076*	Formate:ferredoxin oxidoreductase, α subunit	−5.08 ± 0.08
7	*TK2088*	Membrane-bound hydrogenase, MbhI subunit	−4.76 ± 0.22
8	*TK2087*	Membrane-bound hydrogenase, MbhH subunit	−4.75 ± 0.03
9	*TK2073*	4Fe–4S cluster-binding protein	−4.70 ± 0.01
10	*TK2083*	Membrane-bound hydrogenase, MbhD subunit	−4.66 ± 0.35
11	*TK2081*	Membrane-bound hydrogenase, MbhB subunit	−4.66 ± 0.07
12	*TK2082*	Membrane-bound hydrogenase, MbhC subunit	−4.58 ± 0.06
13	*TK2079*	Probable formate transporter	−4.58 ± 0.03
14	*TK2080*	Membrane-bound hydrogenase, MbhA subunit	−4.54 ± 0.70
15	*TK2091*	Membrane-bound hydrogenase, NiFe-hydrogenase large subunit 2	−4.36 ± 0.22
16	*TK2075*	4Fe–4S cluster-binding protein	−4.01 ± 0.73
17	*TK2085*	Membrane-bound hydrogenase, MbhF subunit	−3.78 ± 0.04
18	*TK2070*	Cytosolic NiFe-hydrogenase, Δ subunit	−3.46 ± 1.39
19	*TK2072*	Cytosolic NiFe-hydrogenase, β subunit	−3.43 ± 0.26
20	*TK2071*	Cytosolic NiFe-hydrogenase, γ subunit	−3.43 ± 0.56
21	*TK2093*	Membrane-bound hydrogenase, 4Fe–4S cluster-binding subunit	−3.11 ± 0.21
22	*TK0039*	Archaeal flagellin B2 precursor	−2.80 ± 0.07
23	*TK0121*	Proline dehydrogenase, Δ subunit (2Fe–2S cluster-binding component)	−2.74 ± 0.10
24	*TK0041*	Archaeal flagellin B4 precursor	−2.67 ± 0.03
25	*TK0043*	Archaeal flagella-related protein C	−2.59 ± 0.03
26	*TK0038*	Archaeal flagellin B1 precursor	−2.56 ± 0.32
27	*TK0044*	Archaeal flagella-related protein D, internal insertion	−2.41 ± 0.16
28	*TK0675*	Hypothetical protein, conserved, radical SAM superfamily	−2.40 ± 0.74
29	*TK0040*	Archaeal flagellin B3 precursor	−2.38 ± 0.28
30	*TK0042*	Archaeal flagellin B5 precursor	−2.22 ± 0.20
31	*TK0631*	Chemotaxis protein methyltransferase	−2.22 ± 0.13
32	*TK0842*	Arsenical-resistance membrane protein	−2.19 ± 0.45
33	*TK0119*	Proline dehydrogenase, α subunit (dye-linked NADH dehydrogenase)	−2.18 ± 0.05
34	*TK1481*	NADH:polysulfide oxidoreductase	−2.18 ± 0.01
35	*TK1209*	Transmembrane electron transport protein	−2.07 ± 0.35
36	*TK1685*	Ferredoxin:NADP oxidoreductase, β subunit	−2.06 ± 0.03
37	*TK0120*	Proline dehydrogenase, Δ subunit (4Fe–4S cluster-binding component)	−2.06 ± 0.28

[a] The mean intensity ratio (DTS/KU216) is expressed as a $\log_2$ value with standard deviation (SD). The *surR* transcript abundance was omitted

analysis was used for further study, as it is regarded as the more accurate method for quantification. Two SBSs were found upstream and downstream of the TATA-Box in both the *FNOR1* and *FNOR2* (hereafter named uSBS1 and dSBS1 for *FNOR1*, and uSBS2 and dSBS2 for *FNOR2*) (Table 4). The distance between the uSBS and the TATA-Box was 19 bp in the *FNOR2*, and 4 bp in the *FNOR1*.

In vivo analyses of the SBSs of *FNOR1* and *FNOR2* genes

To examine the *Tk*-SurR-mediated transcriptional regulation of *FNOR1* and *FNOR2* in vivo, we carried out a reporter analysis using the *Pc-kat* gene, which encodes a thermostable catalase from *P. calidifontis* (Nagaoka et al. 2013). The promoter regions of the *FNOR1* and *FNOR2*

Table 4 Promoter sequences containing a SBS of the genes identified by transcriptome analysis

ORF/Operon	ORF function/description Promoter sequence
Down-regulated in DTS strain ($\log_2$ <−2)	
TK2076–TK2077	Formate dehydrogenase **GTT**AAA**AAC**CAAGCGATTTAAAAACGGTTTTAAGCCAGAAGCGGGAGTTCTGTGT***G***
TK1481	NADH:polysulfide oxidoreductase **GTT**TTA**AAC**CTCGG**GTT**AAGGAAAGTGTTTAATAGTCTTTTGAGAACTCTCTTTGGTGAG GTTAATG
TK1209	Transmembrane electron transport protein **GTT**CTC**AAC**TTTTT**GTT**TTAGAAATCCAGAAAAAAGGACCGTTCCGAGCATACCATC***A***
TK2080–TK2093	Membrane-bound hydrogenase **GTT**CAA**AAC**GAGCC**GTT -N_{39}-** TTTTAAGCAGAATGAGAAATCGGAAGT***G***
TK0675–TK0676	Hypothetical proteins **GTT**TAA**AAC**CTGAG**GTT**AAT**AAC**ATAAG**GTT**CTCAAAAATATTTTAATTTAAGATGGATA ATTGTAATT***G***
TK1684–TK1685	Ferredoxin:$NADP^+$ oxidoreductase (FNOR2) **GTT**CTA**AAC**CTTTG**GTT**CAAAAAAAGCGTATAAACCTTGA**GTT**CAA**AAC**TAAAGGTG***A***
Up-regulated in DTS strain ($\log_2$ >2)	
TK1325–TK1326	Ferredoxin:$NADP^+$ oxidoreductase (FNOR1) **GTT**AAC**AAC**AGGTTTATAAGCACTTAAA**GTT**GTG**AAC**CTTTA***G***

Predicted TATA-Boxes are underlined. SBSs and transcription start sites are shown in bold font and bold italicized font, respectively

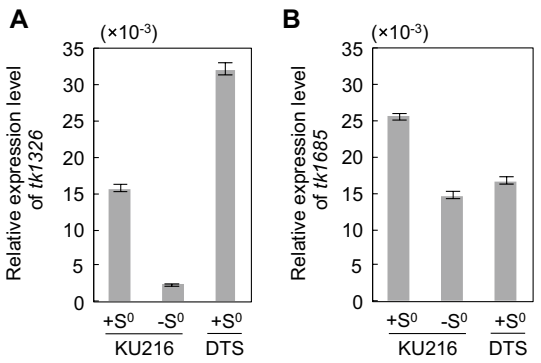

Fig. 1 qRT-PCR analysis of *FNOR*s expression in the KU216 and *Tk*-SurR-deleted strains. Relative transcript abundances of *TK1326* for FNOR1 (**a**) and *TK1685* for FNOR2 (**b**). **a** The relative mRNA expression levels of *TK1326* and *TK1685* were determined by qRT-PCR using total RNA prepared from the KU216 strain cultivated in ASW-YT media containing S^0 or pyruvate ($-S^0$) and the DTS strain cultivated in medium containing S^0 at mid-logarithmic phase. *Error bars* represent standard deviations from three independent experiments. The mRNA levels were normalized to the 16S rRNA level, which was set to 1

were individually fused directly upstream of the *Pc*-Kat gene in the plasmid pTKR (Fig. 2a, b). The resulting plasmids were introduced into the *T. kodakarensis* DAD strain (Δ*pyrF*, Δ*pdaD*) (Fukuda et al. 2008). This strain exhibits agmatine auxotrophy, which is lethal in medium lacking agmatine because an arginine decarboxylase gene is disrupted. By contrast, the DAD strain supplied with the *pdaD* in trans grows in the absence of agmatine, enabling agmatine-based selection of transformants. The expression levels of *Pc*-Kat in DAD cells harboring the corresponding plasmid cultivated in the presence or absence of S^0 are shown in Fig. 2. In DAD cells harboring pTKRF1, *FNOR1* promoter activity was more than fivefold higher in cells grown in the presence of S^0 than in those grown in the absence of S^0, consistent with the corresponding transcript abundance ratio obtained by qRT-PCR (Figs. 1a, 2a). We next introduced point mutations into the individual SBSs to impair binding of *Tk*-SurR. pTKRF1-1 has a defect in uSBS1, pTKRF1-2 in dSBS1, and pTKRF1-12 has defects in both. The transcript levels observed from the variant promoters were comparable to that from pTKRF1 when the cells were grown in the presence of S^0. However, when the cells were grown in the absence of S^0, disturbing the SBSs resulted in transcript levels fivefold higher than that from pTKRF1 grown under the same condition, and equivalent to the levels observed in cells grown with S^0. These results indicated that both consensus sequences (uSBS1 and dSBS1) in the *FNOR1* promoter function as an operator mediating repression by *Tk*-SurR. Interestingly, disturbing a single SBS led to complete derepression, indicating that the individual SBSs cannot repress gene expression alone and that the presence of both SBSs are necessary for repression in vivo.

In the case of *FNOR2*, promoter activity was higher in DAD cells harboring pTKRF2 grown in the presence of S^0 than in cells grown in the absence of S^0, in agreement with the corresponding transcript abundance ratio obtained by qRT-PCR (Figs. 1b, 2b). As in the case of

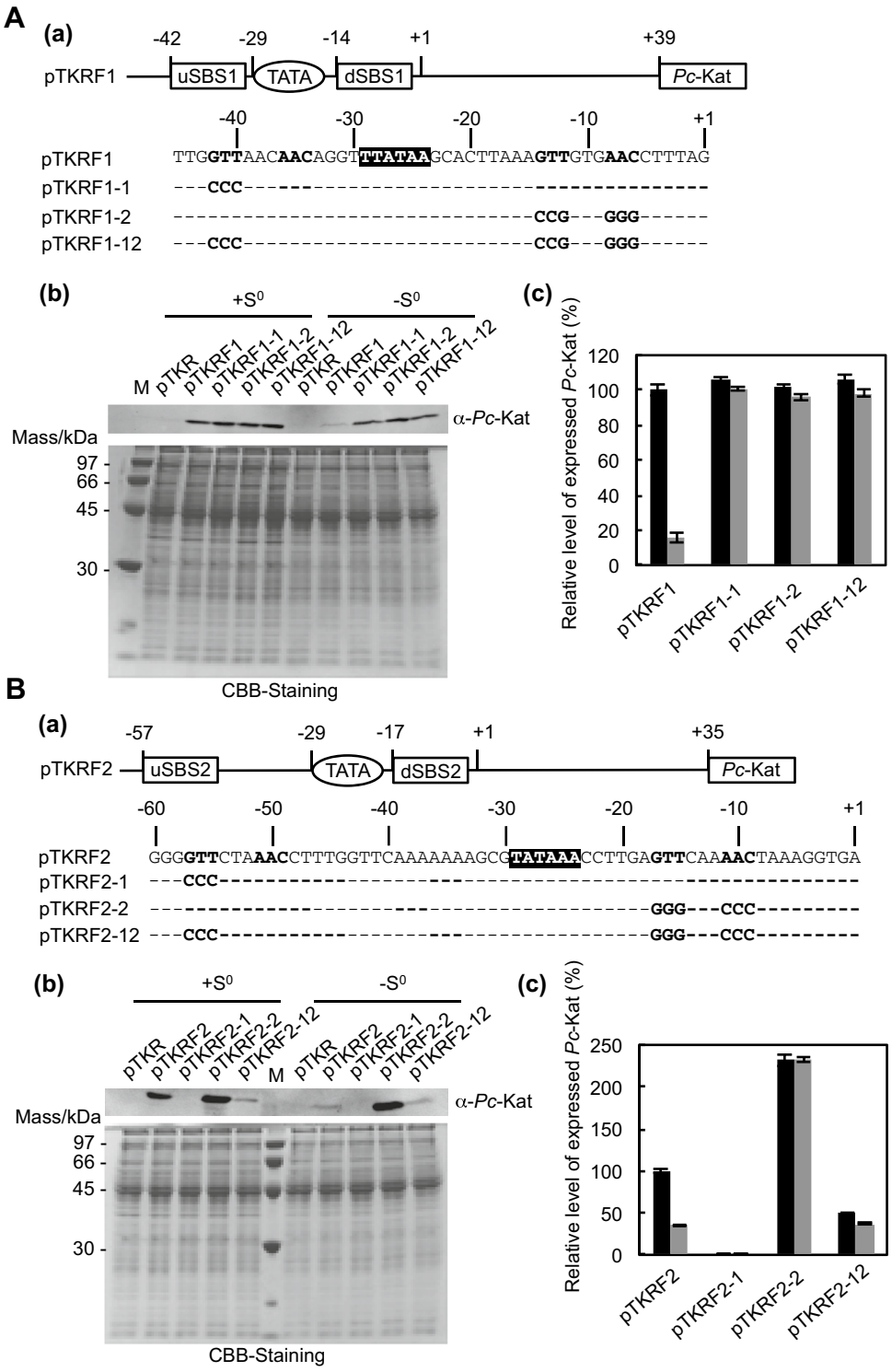

Fig. 2 The roles of SBSs of each *FNOR* promoter region in transcriptional regulation by *Tk*-SurR. **A**-**a** Structural features of the *FNOR* promoter are shown. *+1* indicates the transcriptional start point. The predicted TATA-Box and SBSs are shown in *white letters* and *bold letters*, respectively. **A**-**b** Representative *Pc*-Kat expression patterns in *T. kodakarensis* DAD cells harboring pTKR, pTKRF1, pTKRF1-1, pTKRF1-2, and pTKRF1-12 are shown. Crude extracts (20 μg) of *T. kodakarensis* DAD cells harboring the corresponding plasmids were separated by SDS-PAGE and detected by western blotting using antisera against *Pc*-Kat (*upper*) and Coomassie brilliant blue staining (*lower*) as a loading control. *Lane M*, molecular mass markers. **A**-**c** The values shown indicate the expression level of the *Pc-kat* gene under the control of the native *FNOR1* promoter relative to cells grown in the presence of S^0 (set to 100%). *Black* and *gray bars* represent the *Pc*-Kat levels in cells harboring the corresponding plasmid grown in the presence and absence of S^0, respectively. **B**-**a** Structural features of the *FNOR2* promoter region are shown. **B**-**b** The representative *Pc*-Kat expression patterns in *T. kodakarensis* DAD cells harboring pTKR, pTKRF2, pTKRF2-1, pTKRF2-2, and pTKRF2-12 are shown. **B**-**c** The values shown indicate the expression level of the *Pc-kat* gene under the control of the native *FNOR2* promoter relative to cells grown in the presence of S^0 (set to 100%). All the experiments were performed in triplicate

FNOR1, we introduced mutations into uSBS2 (pTKRF2-1), dSBS2 (pTKRF2-2), or both (pTKRF2-12). Expression from pTKRF2-1 was not detected, irrespective of the presence or absence of S^0, suggesting that uSBS2 functions in a positive manner, enhancing transcription of *FNOR2*. The fact that disturbing uSBS2 still resulted in a decrease in transcript levels in cells grown with S^0 indicates that the reduced form of *Tk*-SurR with binding ability is still present under these growth conditions, at least at a concentration sufficient to bind to uSBS2 and enhance transcription. Expression from pTKRF2-2 was more than 2.5-fold greater than that from pTKRF2

in cells grown in the absence of S^0. This indicates that dSBS2 is involved in repressing the gene expression of *FNOR2* via *Tk*-SurR binding. As the levels of *Pc*-Kat in cells grown with and without S^0 were equivalent, this suggests that the intracellular concentration of the reduced form of *Tk*-SurR is sufficient to trigger maximum activation even in cells grown with S^0, and that the differences in expression levels observed in the presence/absence of S^0 is controlled by the degree of repression brought about by dSBS2. In cells harboring pTKRF2-12, which lacked both SBS2s, a moderate level of expression was observed that showed little response to the presence/absence of S^0. Taken together, the data indicate that uSBS2 functions as an upstream activating site that enhances *FNOR2* transcription, whereas dSBS2 functions as an operator for gene repression. The results also suggest that the activating function of uSBS2 is rather constitutive, and that the overall response of gene expression towards the presence/absence of S^0 is governed by dSBS2.

To further investigate whether the uSBS2 location is essential for the transcription activation, we introduced a uSBS2 cassette (GTTCTAAACCTTTGGTT) 5 bases (pTKRF2-3) or 10 bases (pTKRF2-4) upstream or 5 bases downstream (pTKRF2-5) of the original location of the uSBS2 in *FNOR2* (Fig. 3a). As in the promoter assays described above, the transcription activities of the promoter variants were estimated with *Pc*-Kat in the presence and absence of S^0. As a result, expression from pTKRF2-3, pTKRF2-4, and pTKRF2-5 were not detected, similar to the results of pTKRF2-1 (Fig. 3). This indicates that the location of uSBS2 is crucial for its function in transcriptional activation.

Structural analysis of *Tk*-SurR

Tk-SurR was purified to near homogeneity under aerobic conditions (Fig. 4a). To investigate the binding ability of *Tk*-SurR in response to redox conditions, we carried out a gel-mobility shift assay using a DNA probe amplified from the promoter region in pTKRF2. The band corresponding to the free DNA probe displayed an upward shift with increasing concentrations of *Tk*-SurR reduced by DTT (Fig. 4b), indicating that *Tk*-SurR bound to the promoter of the *FNOR2*, consistent with the finding that the reduced form of *P. furiosus* SurR binds to the SBS (Yang et al. 2010). By contrast, binding was not observed when the DNA probe was incubated with *Tk*-SurR oxidized by the thiol-specific oxidant diamide (Kosower and Kosower 1995). A previous report estimated that approximately 80% of *P. furiosus* SurR is in the reduced state, even when purified aerobically (Yang et al. 2010). Next, we monitored the conformational change between the reduced and oxidized forms of *Tk*-SurR by CD spectrum analysis. The far-UV CD spectra of *Tk*-SurR reduced and oxidized by DTT and diamide, respectively, both showed minimal values at 222 nm, typical for an α-helix (Fig. 4c). However, the value of molecular ellipticity at 222 nm of the reduced form was lower than that of the oxidized form, suggesting that a conformational change of *Tk*-SurR occurred in response to the redox conditions, most likely via the switch of the CXXC motif.

Gel-shift assay

To determine the dissociation constants of *Tk*-SurR bound to the SBSs of the *FNOR1* and *FNOR2* promoters, a

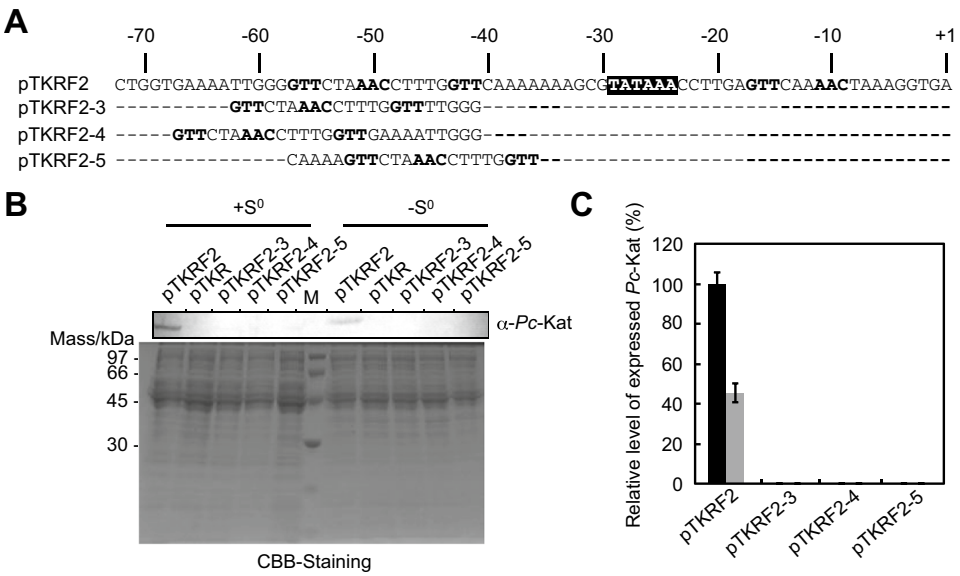

Fig. 3 The importance of the uSBS2 location in *FNOR2* promoter region. **a** Structural variants of the *FNOR2* promoter region are shown. **b** The representative *Pc*-Kat expression patterns in *T. kodakarensis* DAD cells harboring pTKRF2, pTKR, pTKRF2-3, pTKRF2-4, and pTKRF2-5 are shown. **c** The values shown indicate the expression level of the *Pc-kat* gene under the control of the native *FNOR2* promoter relative to cells grown in the presence of S^0 (set to 100%). All the experiments were performed in triplicate

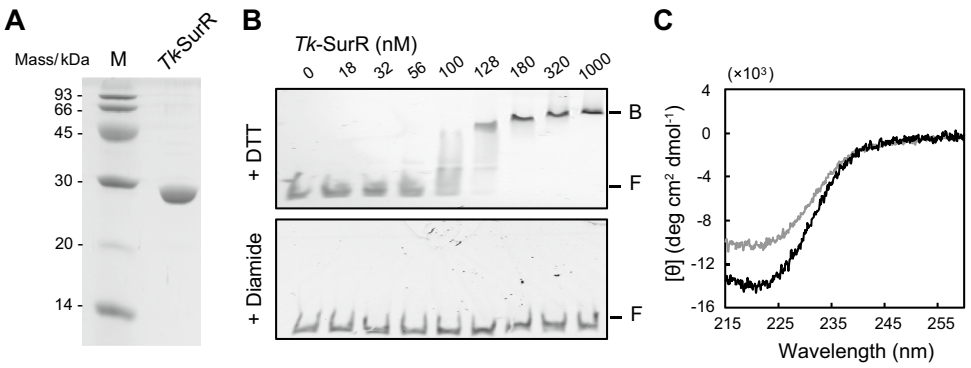

Fig. 4 Binding abilities of the reduced and oxidized forms of *Tk*-SurR to SBS. **a** A 5 µg sample of purified recombinant *Tk*-SurR was separated, and the gel was stained with Coomassie brilliant blue. *Lane M* molecular mass markers. **b** The electrophoretic mobility shift assay showing the ability of the reduced (*upper panel*) and oxidized (*lower panel*) forms of *Tk*-SurR to bind to the native promoter region of the *FNOR2* gene. The protein concentrations used are indicated above *each lane*. The position of bands corresponding to free DNA [F] and bound DNA [B] are shown. **c** Far-UV CD spectra of *Tk*-SurR (1.8 µM) oxidized by 5 mM diamide (*black line*) or reduced by 5 mM DTT (*gray line*) at 20 °C

gel-mobility shift assay was performed using DNA probes amplified from the promoter regions in pTKRF1, pTKRF2, and their variants. This allowed us to examine *Tk*-SurR binding with promoters harboring both SBSs (native in Fig. 5), single SBSs (uSBS, dSBS) and no SBSs (SBS-less). The DNA probe containing the native *FNOR1* promoter displayed a shift with increasing concentrations of *Tk*-SurR (Fig. 5a), indicating that *Tk*-SurR bound to the *FNOR1* promoter as was observed with the *FNOR2* promoter. Next, we determined the apparent dissociation constants by quantitative titrations at a fixed concentration of the probe DNA. The increase in the level of bound DNA with increasing concentrations of *Tk*-SurR was fitted to the Hill equation, yielding apparent dissociation constants of K_d = 283 ± 9 nM for *Tk*-SurR:*FNOR1* promoter and K_d = 189 ± 9 nM for *Tk*-SurR:*FNOR2* promoter (Fig. 5b). The binding affinity of *Tk*-SurR with the *FNOR1* promoter was lower than that with the *FNOR2* promoter. The binding isotherms of *Tk*-SurR to the promoters of the *FNOR1* and *FNOR2* showed a sigmoidal dependence on the protein concentration, with a Hill coefficient of 4.9 ± 0.6 and 3.3 ± 0.4, respectively, indicating that the binding of *Tk*-SurR to each promoter was highly cooperative. No band shifts were observed with the SBS-less probes, confirming that *Tk*-SurR specifically recognized the SBSs in each promoter. When we examined *Tk*-SurR binding with individual SBSs, the dissociation constants were 748 ± 34 nM (*Tk*-SurR:uSBS1), 272 ± 5 nM (*Tk*-SurR:dSBS1), 81 ± 5 nM (*Tk*-SurR:uSBS2) and 116 ± 6 nM (*Tk*-SurR:dSBS2). As predicted from the in vivo experiments, the affinity of *Tk*-SurR for uSBS2 was slightly, but consistently higher than that for dSBS2 in vitro. This supports the assumption that increased binding of *Tk*-SurR to dSBS2 via its reduction governs the regulation of gene expression in *FNOR2*.

Discussion

Here we have carried out in vitro and in vivo analyses on *Tk*-SurR to better understand how the protein regulates gene expression. A conformational change of SurR from *P. furiosus* is considered to occur due to formation of an intramolecular disulfide bond in the CXXC motif in the presence of S^0, thereby forming a DNA-unbound state of the regulator (Yang et al. 2010). Our present CD data also confirmed a structural change of *Tk*-SurR depending on the presence of DTT and diamide (Fig. 4c), and as expected, the oxidized form of *Tk*-SurR did not bind to SBS (Fig. 4b).

Our transcriptome analysis between the DTS strain and KU216 strain revealed a large number of genes under the control of *Tk*-SurR. A much larger number of genes displayed lower levels of transcripts upon *surR* disruption than the number of those that increased (Tables 2, 3). This was also the case with genes that actually harbor an SBS as a *cis*-regulatory element (Table 4). *FNOR1* (*TK1326*) was the only promoter among the up-shifted genes in the DTS strain that contained an SBS. The response of the *mbh* gene cluster to the presence/absence of S^0 has previously been examined, and transcription was rapidly terminated by due to a conformational change of *Tk*-SurR in response to the addition of S^0 (Jäger et al. 2014). In this study, we show that a further decrease in transcript levels of *mbh* was observed with *surR* disruption, even when cells were grown with S^0 (Table 3). In addition, transcripts of *FNOR2* were also detected in the KU216 strain in the presence of S^0 (Fig. 1a). These results suggest that the reduced form of *Tk*-SurR exists to some extent in the cytoplasm even in the presence of S^0, activating (albeit weakly) the expression of genes positively regulated by *Tk*-SurR.

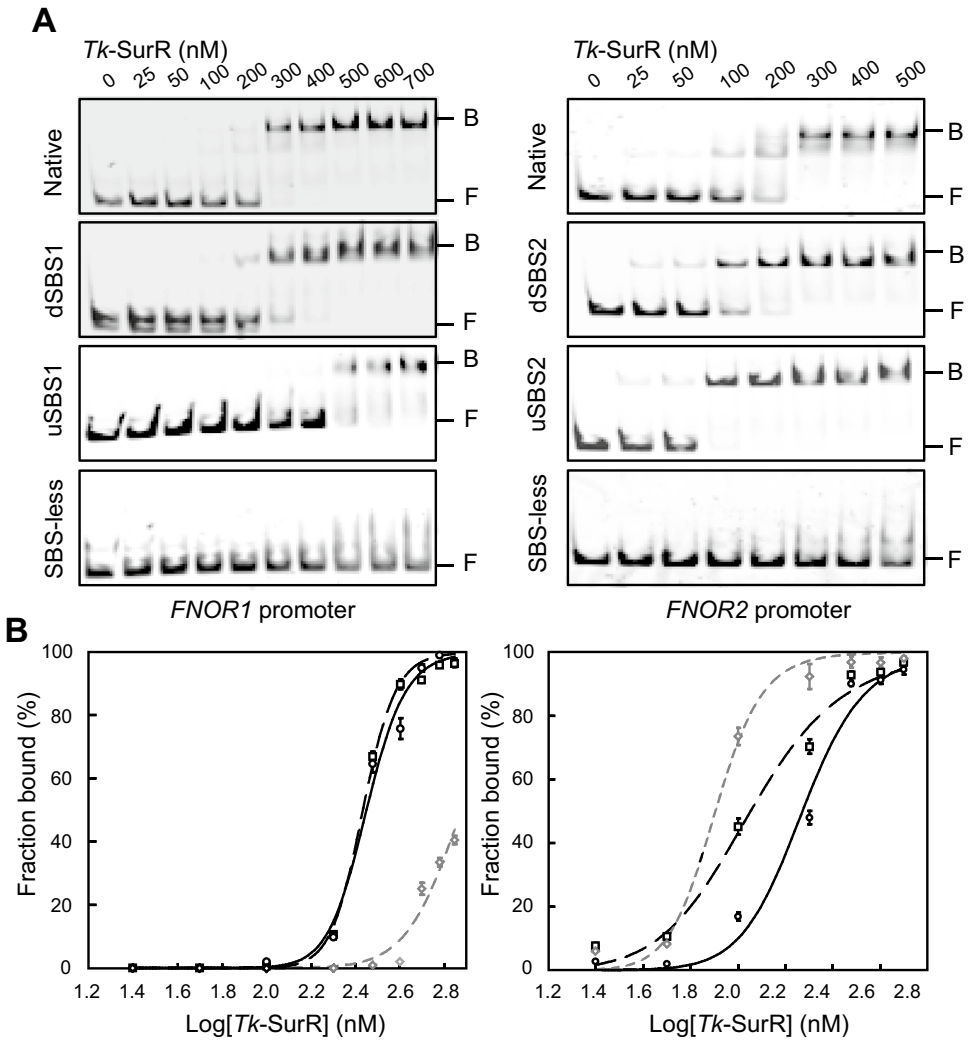

Fig. 5 Binding affinity of *Tk*-SurR to each SBS located in the upstream region of the *FNOR1* and *FNOR2*. **a** The interaction between *Tk*-SurR and different fragments encompassing either the native promoter region of the *FNOR1* (*left panel*), the *FNOR2* (*right panel*), or their SBS mutants (uSBS1, dSBS1, and both SBS1s; uSBS2, dSBS2, and both SBS2s) observed by electrophoretic mobility shift assays. The protein concentrations used are indicated above each *lane*. **b** Binding isotherm; the ratios of the bound DNA fractions quantified by densitometry from the above gel-mobility shift assays are plotted against the concentrations of the *Tk*-SurR dimer. The bound fraction levels shown are from the native promoter region of the FNOR1 gene (*open circle*), dSBS1 (*open square*), and uSBS1 (*open diamond*) (*left panel*), and that of the FNOR2 gene (*open circle*), dSBS2 (*open square*), and uSBS2 (*open diamond*) (*right panel*). *Error bars* represent one standard deviation for each point derived from triplicate experiments

Our results indicate that both uSBS1 and dSBS1 in the *FNOR1* promoter function as an operator mediating repression by *Tk*-SurR. As is the case for *S. solfataricus* Lrs14 (Bell and Jackson 2000) and/or *T. kodakarensis* Tgr (Kanai et al. 2007) and *P. furiosus* Phr (Vierke et al. 2003), the *Tk*-SurR-DNA supercomplex can be presumed to interfere with the binding of TBP and/or TFB to the BRE/TATA-Box and/or the recruitment of RNAP. In the case of *FNOR1*, a single SBS disruption led to complete derepression, indicating that the individual SBSs cannot repress gene expression alone and that the presence of both SBSs is essential for repression in vivo. Disruption of a single SBS (pTKRF1-1 and pTKRF1-2) also abolished the response of gene expression towards S^0 (Fig. 2a), indicating that both uSBS1 and dSBS1 are needed for the response. The cooperative behaviors of the two SBSs in vivo are also supported by the binding assays carried out in vitro. If the two sites were recognized completely independently, we should observe band shifts in two concentration ranges in Fig. 5a (*FNOR1* promoter, left panel), as *Tk*-SurR binding to dSBS1 (300 nM) and uSBS1 (500 nM) occur at different concentration ranges. However, the band shift with the native promoter (with dSBS1 and uSBS1) predominantly occurs at the same concentration range as that with the promoter with only dSBS1. Furthermore, this band displays lower mobility than the shifted bands observed with probes with single SBSs (data not shown), indicating that the band represents a probe bound by *Tk*-SurR at both SBSs. Taken together, we can presume that *Tk*-SurR binding to dSBS1 promotes binding of *Tk*-SurR to uSBS1 in a cooperative manner.

In the case of *FNOR2*, our data indicate that uSBS2 functions as an upstream activating site that enhances *FNOR2* transcription, whereas dSBS2 functions as an operator for gene repression. The results also suggest that the activating function of uSBS2 is rather constitutive, and that the overall response of gene expression towards the presence/absence of S^0 is regulated by the binding or release of *Tk*-SurR to dSBS2. *Tk*-SurR bound to uSBS2 of *FNOR2* more efficiently than to dSBS2 in vitro, which

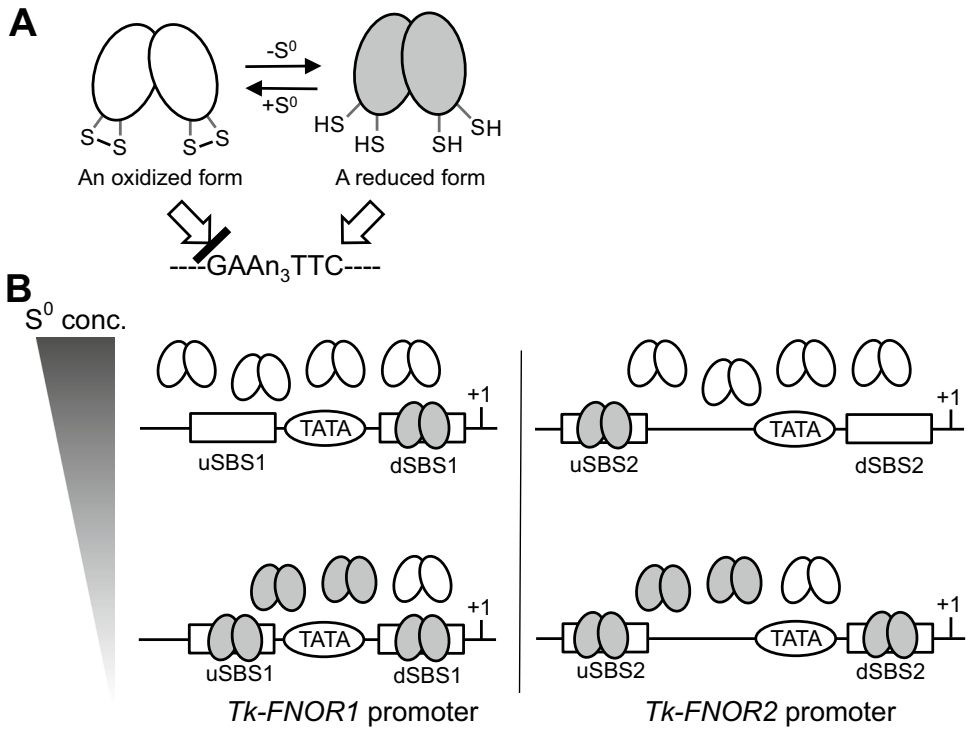

Fig. 6 A proposed model of *FNOR*s expression regulation by *Tk*-SurR. **a** The conformations of *Tk*-SurR in the presence and absence of S^0. The two cysteine residues in the CXXC motif of *Tk*-SurR form an intramolecular disulfide bond in the presence of S^0. A reduced form of SurR in the absence of S^0 binds to the SBS ($GAAn_3TTC$). **b** At a low S^0 concentration or in the absence of S^0, a large amount of reduced *Tk*-SurR (*shaded circles*) would bind to SBS to regulate gene expression. The reduced form is gradually oxidized (*white circles*) with an increasing amount of S^0 in the medium, resulting in the formation of a DNA-unbound state. However, a small amount of the reduced form is still involved in gene regulation even in the presence of S^0. In transcriptional regulation of *FNOR1* expression, both uSBS1 and dSBS1 function as an operator for gene repression upon *Tk*-SurR binding. The binding of *Tk*-SurR to uSBS1 will trigger strong repression of *FNOR1* expression. On the other hand, uSBS2 and dSBS2 act as the upstream activating site and operator for gene activation and repression upon *Tk*-SurR binding, respectively, in the regulation of *FNOR2* expression. The binding of *Tk*-SurR to dSBS2 reduces excessive expression of the *FNOR2*

may explain why *Tk*-SurR overall enhances *FNOR2* transcription. We also revealed that the position of uSBS2 is important for the site to act as an activating element. Shifting uSBS2 5 bp upstream or downstream completely abolished the activating effect of the SBS. As the double helix of B-DNA is right-handed with about 10–10.5 base pairs per turn, a 5-base shift in location can be considered to change the accessible surface for *Tk*-SurR. However, a 10-base shift upstream also abolished the activating effect. Although further analyses are necessary to determine the importance of the orientation of the uSBS2 relative to the TATA-Box, our results indicate that the position of uSBS2 is important for the transcriptional activation. A kinetic study using a gel-shift assay showed that the dissociation constant of *Tk*-SurR was slightly lower for uSBS2 ($K_d = 81 \pm 5$ nM) than for dSBS2 ($K_d = 116 \pm 6$ nM) (Fig. 5b). These results suggest that preferential binding of a small amount of the reduced form of *Tk*-SurR to uSBS2 enables induction of *FNOR2* expression, whereas expression is gradually repressed by binding of *Tk*-SurR to dSBS2 as the concentration of reduced *Tk*-SurR increases (Fig. 6). A transcriptional activator, TFB-RF1, supports the transcription of a gene with a weak BRE for efficient activation. The BRE sequence is considered to be not only a determinant of the direction of transcription, but also a key factor in stabilizing the TFB–TBP–RNA polymerase complex (Ochs et al. 2012). We speculate that *Tk*-SurR recruits TFB to the BRE sequence of the *FNOR2* to stabilize the transcription initiation complex to activate transcription. The results of this study raise the possibility that the location of the SBS as well as the binding affinity of *Tk*-SurR for the SBS are key determinants for controlling the expression of genes under *Tk*-SurR control.

It is unclear why two *FNOR*s are present on *T. kodakarensis* genome. Most archaea belonging to the order Thermococcales contain two kinds of *FNOR*s on the genomes, and SBSs are located in their predicted promoter regions (Fig. 7). These archaea are all S^0-reducing organisms and possess *Tk*-SurR orthologs. It is likely that the expressions

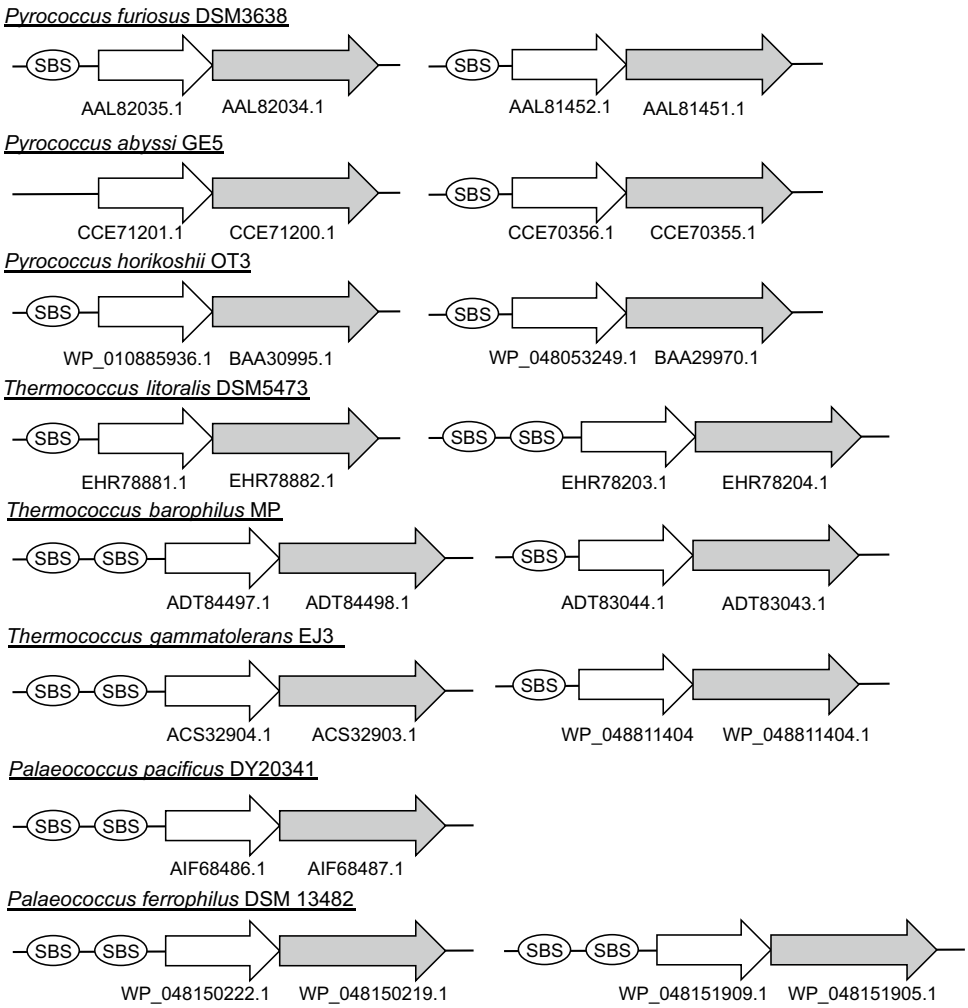

Fig. 7 Distribution of FNOR orthologues in the order Thermococcales. Clustering of FNOR α- and β-subunit genes in the genomes of the order Thermococcales. *White* and *gray arrows* indicate the ORFs for FNOR α- and β-subunits, respectively. Protein accession numbers of GenBank or NCBI reference sequence are displayed below the ORFs. SBSs ($GTTn_3AAC$) located within 100 bp upstream of each start codon sequence are shown in *circle*

of *FNOR*s are mainly under the regulation of *Tk*-SurR in response to S^0, as in the case of *T. kodakarensis*.

Acknowledgements This study was supported by a Grant from the Japan Society for the Promotion of Science (JSPS) KAKENHI (26292045) to S.F. and KAKENHI (17H05027) to R.H. Bioinformatic analysis was supported by a Grant for Individual Special Research, provided by Kwansei-Gakuin University.

References

Amo T, Atomi H, Imanaka T (2002) Unique presence of a manganese catalase in a hyperthermophilic archaeon, *Pyrobaculum calidifontis* VA1. J Bacteriol 184:3305–3312. doi:10.1128/JB.184.12.3305-3312.2002

Antelmann H, Helmann JD (2011) Thiol-based redox switches and gene regulation. Antioxid Redox Signal 14:1049–1063. doi:10.1089/ars.2010.3400

Atomi H, Fukui T, Kanai T, Morikawa M, Imanaka T (2004) Description of *Thermococcus kodakaraensis* sp. nov., a well studied hyperthermophilic archaeon previously reported as *Pyrococcus* sp. KOD1. Archaea 1:263–267. doi:10.1155/2004/204953

Bell SD, Jackson SP (2000) Mechanism of autoregulation by an archaeal transcriptional repressor. J Biol Chem 275:31624–31629. doi:10.1074/jbc.M005422200

Blombach F, Smollett KL, Grohmann D, Werner F (2016) Molecular mechanisms of transcription initiation—structure, function, and evolution of TFE/TFIIE-like factors and open complex formation. J Mol Biol 428:2592–2606. doi:10.1016/j.jmb.2016.04.016

Bradford MM (1976) A rapid and sensitive method for the quantitation of microgram quantities of protein utilizing the principle of protein–dye binding. Anal Biochem 72:248–254. doi:10.1016/0003-2697(76)90527-3

Fiala G, Stetter KO (1986) *Pyrococcus furiosus* sp. nov. represents a novel genus of marine heterotrophic archaebacteria growing optimally at 100 °C. Arch Microbiol 145:56–61. doi:10.1007/BF00413027

Fukuda W, Morimoto N, Imanaka T, Fujiwara S (2008) Agmatine is essential for the cell growth of *Thermococcus kodakaraensis*. FEMS Microbiol Lett 287:113–120. doi:10.1111/j.1574-6968.2008.01303.x

Geiduschek EP, Ouhammouch M (2005) Archaeal transcription and its regulators. Mol Microbiol 56:1397–1407. doi:10.1111/j.1365-2958.2005.04627.x

Gindner A, Hausner W, Thomm M (2014) The TrmB family: a versatile group of transcriptional regulators in Archaea. Extremophiles 18:925–936. doi:10.1007/s00792-014-0677-2

Grohmann D, Werner F (2011) Recent advances in the understanding of archaeal transcription. Curr Opin Microbiol 14:328–334. doi:10.1016/j.mib.2011.04.012

Hillion M, Antelmann H (2015) Thiol-based redox switches in prokaryotes. Biol Chem 396:415–444. doi:10.1515/hsz-2015-0102

Jäger D, Förstner KU, Sharma CM, Santangelo TJ, Reeve JN (2014) Primary transcriptome map of the hyperthermophilic archaeon *Thermococcus kodakarensis*. BMC Genom 15:684. doi:10.1186/1471-2164-15-684

Johnsen U, Sutter JM, Schulz AC, Tästensen JB, Schönheit P (2015) XacR—novel transcriptional regulator of D-xylose and L-arabinose catabolism in the haloarchaeon *Haloferax volcanii*. Environ Microbiol 17:1663–1676. doi:10.1111/1462-2920.12603

Jun SH, Reichlen MJ, Tajiri M, Murakami KS (2011) Archaeal RNA polymerase and transcription regulation. Crit Rev Biochem Mol Biol 46(1):27–40. doi:10.3109/10409238.2010.538662

Kanai T, Akerboom J, Takedomi S, van de Werken HJ, Blombach F, van der Oost J, Murakami T, Atomi H, Imanaka T (2007) A global transcriptional regulator in *Thermococcus kodakaraensis* controls the expression levels of both glycolytic and gluconeogenic enzyme-encoding genes. J Biol Chem 282:33659–33670. doi:10.1074/jbc.M703424200

Koltai H, Weingarten-Baror C (2008) Specificity of DNA microarray hybridization: characterization, effectors and approaches for data correction. Nucleic Acids Res 36:2395–2405. doi:10.1093/nar/gkn087

Kosower NS, Kosower EM (1995) Diamide: an oxidant probe for thiols. Methods Enzymol 251:123–133. doi:10.1016/0076-6879(95)51116-4

Leyn SA, Rodionov DA (2015) Comparative genomics of DtxR family regulons for metal homeostasis in Archaea. J Bacteriol 197:451–458. doi:10.1128/JB.02386-14

Lim JK, Jung HC, Kang SG, Lee HS (2017) Redox regulation of SurR by protein disulfide oxidoreductase in *Thermococcus onnurineus* NA1. Extremophiles 21:491–498. doi:10.1007/s00792-017-0919-1

Lipscomb GL, Keese AM, Cowart DM, Schut GJ, Thomm M, Adams MW, Scott RA (2009) SurR: a transcriptional activator and repressor controlling hydrogen and elemental sulphur metabolism in *Pyrococcus furiosus*. Mol Microbiol 71:332–349. doi:10.1111/j.1365-2958.2008.06525.x

Lipscomb GL, Schut GJ, Scott RA, Adams MWW (2017) SurR is a master regulator of the primary electron flow pathways in the order Thermococcales. Mol Microbiol. doi:10.1111/mmi.13668

Liu H, Orell A, Maes D, van Wolferen M, Lindås AC, Bernander R, Albers SV, Charlier D, Peeters E (2014) BarR, an Lrp-type transcription factor in *Sulfolobus acidocaldarius*, regulates an aminotransferase gene in a β-alanine responsive manner. Mol Microbiol 92:625–639. doi:10.1111/mmi.12583

Matsumi R, Manabe K, Fukui T, Atomi H, Imanaka T (2007) Disruption of a sugar transporter gene cluster in a hyperthermophilic archaeon using a host-marker system based on antibiotic resistance. J Bacteriol 189:2683–2691. doi:10.1128/JB.01692-06

Nagaoka E, Hidese R, Imanaka T, Fujiwara S (2013) Importance and determinants of induction of cold-induced DEAD RNA helicase in the hyperthermophilic archaeon *Thermococcus kodakarensis*. J Bacteriol 195:3442–3450. doi:10.1128/JB.00332-13

Ochs SM, Thumann S, Richau R, Weirauch MT, Lowe TM, Thomm M, Hausner W (2012) Activation of archaeal transcription mediated by recruitment of transcription factor B. J Biol Chem 287:18863–18871. doi:10.1074/jbc.M112.365742

Reeve JN (2003) Archaeal chromatin and transcription. Mol Microbiol 48:587–598. doi:10.1046/j.1365-2958.2003.03439.x

Santangelo TJ, Cubonová L, Reeve JN (2008) Shuttle vector expression in *Thermococcus kodakaraensis*: contributions of *cis* elements to protein synthesis in a hyperthermophilic archaeon. Appl Environ Microbiol 74:3099–3104. doi:10.1128/AEM.00305-08

Santangelo TJ, Cuboňová L, Reeve JN (2011) Deletion of alternative pathways for reductant recycling in *Thermococcus kodakarensis* increases hydrogen production. Mol Microbiol 81:897–911. doi:10.1111/j.1365-2958.2011.07734.x

Sato T, Fukui T, Atomi H, Imanaka T (2003) Targeted gene disruption by homologous recombination in the hyperthermophilic archaeon *Thermococcus kodakaraensis* KOD1. J Bacteriol 185:210–220. doi:10.1128/JB.185.1.210-220.2003

Sato T, Fukui T, Atomi H, Imanaka T (2005) Improved and versatile transformation system allowing multiple genetic manipulations of the hyperthermophilic archaeon *Thermococcus kodakaraensis*. Appl Environ Microbiol 71:3889–3899. doi:10.1128/AEM.71.7.3889-3899.2005

Schulz S, Gietl A, Smollett K, Tinnefeld P, Werner F, Grohmann D (2016) TFE and Spt4/5 open and close the RNA polymerase clamp during the transcription cycle. Proc Natl Acad Sci USA 113:E1816–E1825. doi:10.1073/pnas.1515817113

Soler N, Justome A, Quevillon-Cheruel S, Lorieux F, Le Cam E, Marguet E, Forterre P (2007) The rolling-circle plasmid pTN1 from the hyperthermophilic archaeon *Thermococcus nautilus*. Mol Microbiol 66:357–370. doi:10.1111/j.1365-2958.2007.05912.x

Vierke G, Engelmann A, Hebbeln C, Thomm M (2003) A novel archaeal transcriptional regulator of heat shock response. J Biol Chem 278:18–26. doi:10.1074/jbc.M209250200

Werner F, Grohmann D (2011) Evolution of multisubunit RNA polymerases in the three domains of life. Nat Rev Microbiol 9:85–98. doi:10.1038/nrmicro2507

Yang H, Lipscomb GL, Keese AM, Schut GJ, Thomm M, Adams MW, Wang BC, Scott RA (2010) SurR regulates hydrogen production in *Pyrococcus furiosus* by a sulfur-dependent redox switch. Mol Microbiol 77:1111–1122. doi:10.1111/j.1365-2958.2010.07275.x